Journal of Computational and Applied Mathematics 46 (1993) 49–64
North-Holland

CAM 1327

A Fornberg-like conformal mapping method for slender regions

Thomas K. DeLillo * and Alan R. Elcrat **

Department of Mathematics and Statistics, Wichita State University, Wichita, KS, United States

Received 18 October 1991
Revised 18 February 1992

Abstract

DeLillo, T.K. and A.R. Elcrat, A Fornberg-like conformal mapping method for slender regions, Journal of Computational and Applied Mathematics 46 (1993) 49–64.

A method is presented for approximating the conformal map from the interior of an ellipse to the interior of a simply-connected target region. The map is represented as a truncated Chebyshev series. Conditions that the mapping function be conformal are transplanted from the ellipse to an annulus with the Joukowski map. The resulting conditions on the Laurent coefficients then give a system of equations for the Newton update of the approximate boundary correspondence. This system is a generalization of Fornberg's system for maps from the disk and is solved similarly in $O(N \log N)$ operations by the conjugate gradient method. Our numerical experiments demonstrate that the maps from the ellipse to a slender target region of similar aspect ratio can be constructed with far fewer mesh points than are required for maps from the disk, thus circumventing the ill-conditioning due to crowding in these cases.

Keywords: Numerical conformal mapping; Fornberg's method; Chebyshev series; crowding.

0. Introduction

In the extensive efforts to give a constructive and computational realization to the Riemann mapping theorem a central role has been given to finding the map from the unit disk to a domain bounded by a Jordan curve. One reason for this is the natural role played by the Taylor series for the mapping function inside the disk and the associated Fourier series on the boundary. The classic exposition of the development of ideas connected with this is given in [6, Chapter 2]. More recently the Fourier series methods have been given a new perspective with the introduction of the use of the Fast Fourier Transform (FFT) algorithm to compute

Correspondence to: Prof. T.K. DeLillo, Department of Mathematics and Statistics, Wichita State University, Wichita, KS 67260-0033, United States.

* This author's research was partially supported by U.S. Department of Energy grant DE-FG02-92ER25124 and NSF grant OSR-9255223, NSF EPSCoR program.

** This author's research was partially supported by U.S. Air Force grant AFSOR 89-0323 and NSF grant OSR-9255223, NSF EPSCoR program.

0377-0427/93/$06.00 © 1993 – Elsevier Science Publishers B.V. All rights reserved

discretizations of the conjugation operator (see [8]). The rapid expansion of computational power together with the use of FFTs made it possible to attempt much more ambitious problems than had been considered before. In some applications, e.g., time-dependent hydrodynamic calculations, problems were encountered in which the global properties of the domain required a very large number of Fourier coefficients for an accurate solution. In particular, the map to a region which is slender in one direction has relative distortions which vary exponentially with the "aspect ratio", hence the requirement of many Fourier components for resolution. This has come to be known as the *crowding phenomenon* [2,10,18]. For a 5-to-1 ellipse the map is difficult to compute. In a related phenomenon the Schwarz–Christoffel map for a 10-to-1 rectangle becomes nearly impossible. The suggestion that the disk is not a good canonical domain to use for such domains is natural. (In the case of thin polygonal domains this suggestion has been acted on by Howell and Trefethen [10], and they have used infinite strips and thin rectangles successfully for problems that could not have been done before.) The purpose of this work is to show how to deal with a smooth region elongated in one direction by using an ellipse with a similar aspect ratio. The map will be represented as a truncated Chebyshev series whose coefficients are computed using ideas analogous to Fornberg's method for maps from the disk. Our numerical method is essentially a Newton method for finding the boundary correspondence from the ellipse to the region. Wegmann [13] has shown that such Newton methods converge if the initial guess is close enough.

The main question to be dealt with here is how to give a discretization which leads to linear equations which can be solved efficiently and which resolve the map with a modest number of terms. Fornberg [5] solved the linear equations in a Newton step by projecting a function on the circle into the Hardy space of functions analytic in the interior. We will use the same idea except that functions analytic inside the ellipse are represented by the Faber series for this curve, the Faber polynomials being here the Chebyshev polynomials. A function defined on the ellipse decomposes into a sum of functions analytic inside and outside, respectively; the projection can be represented in terms of Laurent coefficients of the transplantation to an annulus by the Joukowski map. The discretization of the projection equation can be solved efficiently using FFTs to implement the conjugate gradient method for a related system of equations.

An outline of the paper is as follows. In Section 1 we review the Newton method to be used. In Section 2 the equations to be solved in making a Newton step are derived. In Section 3 the discretization and associated linear algebra is given. In Section 4 numerical examples are presented. In Section 5 theoretical questions and possible extensions are discussed.

1. Newton's method

Suppose that f is a conformal map from the domain D in the z-plane, bounded by the Jordan curve C, to the domain Ω in the w-plane, bounded by the Jordan curve Γ. Assume that both D and Ω contain the origin. Suppose further that C is described by a function $z(\theta)$, $0 \leqslant \theta \leqslant 2\pi$, and Γ by $\gamma(s)$, s being arc length along Γ, and that z, γ are Hölder continuously differentiable with nonvanishing derivatives. The normalizations $f(0) = 0$ and $f(z(0)) = \gamma(0)$ uniquely determine f; further, finding f is equivalent to finding the function $s(\theta)$ such that $f(z(0)) := \xi(\theta) = \gamma(s(\theta))$. This function is called the *boundary correspondence*. Most methods for

constructing f are methods for finding $s(\theta)$ (or its inverse); we will use one which may be thought of as Newton's method for the nonlinear singular integral equation

$$\frac{1}{2\pi \mathrm{i}} \int_C \frac{\gamma(S(\zeta))}{\zeta - z}\, \mathrm{d}\zeta = \tfrac{1}{2}\gamma(S(z)), \quad z \in C,$$

for $S(z) = S(z(\theta)) = S(\theta)$. More precisely, if $S_k(\theta)$ is known, we determine $U_k(\theta) = S_{k+1}(\theta) - S_k(\theta)$ by the condition that $\xi(\theta) + \mathrm{e}^{\mathrm{i}\beta(\theta)} U_k(\theta)$, $\xi(\theta) = \gamma(S_k(\theta))$, $\beta(\theta) = \arg \gamma'(S_k(\theta))$, extends into D as an analytic function continuous on $D \cup C$ which vanishes at the origin. This function is a conformal map onto a (hopefully) nearby domain $\tilde{\Omega}$. The function $S_{k+1}(\theta)$ is then taken to be the new approximation to the boundary correspondence; the boundary normalizations of the approximate maps are guaranteed by choosing $U_k(0) = 0$. Wegmann has proven that this "equation" for U always has a unique solution, and that if the curves are twice Lipschitz continuously differentiable, this iteration converges for an initial guess which is close enough in a Hölder norm [13]. Two closely related numerical methods for implementing this iteration have been given in [5] and in [13,14] for the case in which D is the unit disk. Fourier analysis plays a central role in these works and the difference lies mainly in the method used to solve the discrete version of the Newton update equation. In [14], it was shown that the discrete iterations follow the continuous ones for a fine enough discretization. It seems clear that such a theorem should hold also in the generality described above for a reasonable discretization.

The purpose of this section has been to recall the basic idea of the Newton method for the boundary correspondence and to explicitly point out that Wegmann's original convergence proof does not require that D be the unit disk.

2. Fourier analysis of Newton update equations

We will use as our canonical domain the ellipse E in the z-plane given by

$$z(\theta) = \tfrac{1}{2}(\rho \mathrm{e}^{\mathrm{i}\theta} + \rho^{-1}\mathrm{e}^{-\mathrm{i}\theta}), \quad 0 \leqslant \theta \leqslant 2\pi,$$

where $\rho > 1$; this is the image of the circle $|t| = \rho$ under the Joukowski map

$$z = \tfrac{1}{2}(t + t^{-1}) = \psi(t),$$

with inverse

$$t = \varphi(z) = z + \sqrt{z^2 - 1}\,.$$

We want to find f conformal in the interior of E mapping to a region of similar aspect ratio normalized by $f(0) = 0$, $f(\frac{1}{2}(\rho + \rho^{-1})) = \gamma(0)$.

Essential use will be made of the expansion of functions analytic inside E in terms of Chebyshev polynomials:

$$f(z) = \sum_{k=0}^{\infty}{}' A_k T_k(z) = \tfrac{1}{2}A_0 + \sum_{k=1}^{\infty} A_k T_k(z),$$

where

$$T_k(z) = \cos(k \arccos(z)) = \tfrac{1}{2}(t^k + t^{-k}).$$

Since $\{T_k(z)\}$ are the Faber polynomials for this domain, this is the natural expansion to use, and the coefficients are given by [7], [8, Chapter 18]

$$A_k = \frac{1}{\pi \mathrm{i}} \int_E \frac{\varphi'(s)}{(\varphi(s))^{k+1}} f(s)\, \mathrm{d}s, \quad k \geqslant 0.$$

If we write $g(t) = f(\psi(t))$, $1 \leqslant |t| \leqslant \rho$, then

$$A_k = 2\rho^{-k} a_k, \quad k \geqslant 0,$$

where $\{a_k\}$ are the Laurent coefficients of g. Suppose now we consider a function h defined on E. For simplicity we assume that h is Lipschitz continuous on E. Together with $h(z)$ we consider the function defined on $\zeta = \mathrm{e}^{\mathrm{i}\theta}$ by transplantation and denote it also by $h(\zeta)$. Then $h(z)$ extends to an analytic function inside E if and only if [8, p.114]

$$\int_E h(z) T_k(z)\, \mathrm{d}z = 0, \quad k \geqslant 0.$$

This is equivalent to

$$\begin{aligned} 0 &= \int_{|\zeta|=1} h(\zeta) \tfrac{1}{2}(\rho^k \zeta^k + \rho^{-k}\zeta^{-k}) \tfrac{1}{2}(1 - \rho^{-2}\zeta^{-2}) \rho\, \mathrm{d}\zeta \\ &= \tfrac{1}{4}\mathrm{i} \int_0^{2\pi} h(\mathrm{e}^{\mathrm{i}\theta}) \big[(\rho^{k+1} \mathrm{e}^{\mathrm{i}(k+1)\theta} - \rho^{-(k+1)} \mathrm{e}^{-\mathrm{i}(k+1)\theta}) \\ &\qquad - (\rho^{k-1} \mathrm{e}^{\mathrm{i}(k-1)\theta} - \rho^{-(k-1)} \mathrm{e}^{-\mathrm{i}(k-1)\theta}) \big]\, \mathrm{d}\theta, \end{aligned}$$

that is,

$$\rho^{k+1} a_{-(k+1)} - \rho^{-(k+1)} a_{k+1} = \rho^{k-1} a_{-(k-1)} - \rho^{-(k-1)} a_{k-1}.$$

These equations can be solved inductively and the result is

$$a_{-k} = \rho^{-2k} a_k, \quad k \geqslant 0. \tag{2.1}$$

We write

$$h(\zeta) = \sum_{-\infty}^{\infty} a_k \zeta^k = \sum_{k=1}^{\infty} a_k \zeta^k + \sum_{k=0}^{\infty} a_{-k} \zeta^{-k} = h_1(\zeta) + h_2(\zeta).$$

Then (2.1) can be written as

$$h_2(\zeta) = h_1\left(\frac{1}{\rho^2 \zeta}\right) + a_0. \tag{2.2}$$

We write, as in [15],

$$h_1 = P_+ h = \tfrac{1}{2}(I + \mathrm{i}K - J)h, \qquad h_2 = P_- h = \tfrac{1}{2}(I - \mathrm{i}K + J)h,$$

where K is the conjugation operator

$$Kh(\theta) = \frac{1}{2\pi}\, \mathrm{PV} \int_0^{2\pi} \cot(\tfrac{1}{2}(\theta - \phi)) h(\phi)\, \mathrm{d}\phi,$$

and

$$Jh(\theta) = a_0 = \frac{1}{2\pi}\int_0^{2\pi} h(\theta)\,\mathrm{d}\theta.$$

Then (2.2) can be written as

$$P_-h = Cl * P_+h + Jh, \tag{2.3}$$

where $C(\mathrm{e}^{\mathrm{i}k\theta}) = \mathrm{e}^{-\mathrm{i}k\theta}$, $*$ denotes convolution and

$$l(\theta) = \sum_{k=0}^{\infty} \rho^{-2k}\mathrm{e}^{\mathrm{i}k\theta} = \frac{1}{1-\rho^{-2}\mathrm{e}^{\mathrm{i}\theta}}.$$

This is an operator equation which may be described conveniently using infinite matrices acting on the Fourier coefficients of h. If $h = h(\theta)$ and $Fh = (\ldots, \hat{h}_1, \hat{h}_0, \hat{h}_{-1}, \ldots)^{\mathrm{T}}$, then

$$l * h = F^{-1}\Lambda Fh,$$

where

$$\Lambda = \begin{bmatrix} \ddots & & & & & & \iddots \\ & \rho^{-4} & & & & 0 & \\ & & \rho^{-2} & & 0 & & \\ & & & 1 & & & \\ & & 0 & & 0 & & \\ & 0 & & & & 0 & \\ \iddots & & & & & & \ddots \end{bmatrix},$$

for example. If we write $L = Cl * P_+ + J = F^{-1}\hat{L}F$, then with

$$\hat{L} = \begin{bmatrix} \ddots & & & & & & \iddots \\ & 0 & & & & 0 & \\ & & 0 & & 0 & & \\ & & & 1 & & & \\ & & \rho^{-2} & & 0 & & \\ & \rho^{-4} & & & & 0 & \\ \iddots & & & & & & \ddots \end{bmatrix},$$

(2.3) can be written $(\hat{P} - \hat{L})Fh = 0$, where $P_- = F^{-1}\hat{P}F$, and where

$$\hat{P} - \hat{L} = \begin{bmatrix} \ddots & & & & & & \iddots \\ & 0 & & & & 0 & \\ & & 0 & & 0 & & \\ & & & 0 & & & \\ & & -\rho^{-2} & & 1 & & \\ & -\rho^{-4} & & & & 1 & \\ \iddots & & & & & & \ddots \end{bmatrix}.$$

The Newton step equation, which requires that $\xi + e^{i\beta}U$ extend to a function analytic inside E, can be written then as

$$(\hat{P}-\hat{L})F(e^{i\beta}U) = -(\hat{P}-\hat{L})F\xi. \tag{2.4}$$

In order to determine U, additional equations are required. For one thing no use has been made of the fact that U is real. In addition, the normalization condition on $f(z)$ that $f(0)=0$ requires that

$$0 = f(0) = \tfrac{1}{2}A_0 + \sum_{k=1}^{\infty}(-1)^k A_{2k} = a_0 + 2\sum_{k=1}^{\infty}(-1)^k \rho^{-2k} a_{2k}, \tag{2.5}$$

since $T_{2k}(0) = (-1)^k$, $T_{2k+1}(0) = 0$, and $2a_k\rho^{-k} = A_k$. We may think of this condition as replacing the one which corresponds to the middle row (of zeros) in the matrix $\hat{P}-\hat{L}$ in (2.4). An equation similar to (2.4) can be obtained by taking complex conjugates and using the fact that U is real. This may be thought of as providing an infinite system in which "the count is right". On the other hand, we expect the associated operator to have a one-dimensional null space since the normalization condition $U(0)=0$ has not yet been applied. In the case of Fornberg's method, clarification of this issue is a central theme of [15].

3. Discretization

We discretize (2.4) using N Fourier points $\theta_k = 2\pi k/N$, N even, with $U_N = [u_0, u_1, \ldots, u_{N-1}]^{\mathrm{T}}$, F_N the N-point discrete Fourier transform, and $\hat{a} = [\hat{a}_{N/2}, \ldots, \hat{a}_1, \hat{a}_0, \hat{a}_{-1}, \ldots, \hat{a}_{-N/2+1}]^{\mathrm{T}} = F_N a$. Equation (2.4) is then replaced by

$$(\hat{P}-\hat{L})_N F_N E_N U_N = -(\hat{P}-\hat{L})_N F_N \xi_N, \tag{3.1}$$

where $E_N = \mathrm{diag}(e_0, \ldots, e_{N-1})$, $e_k = e^{i\beta(\theta_k)}$, and

$$(\hat{P}-\hat{L})_N \hat{a} = \begin{bmatrix} 0 & & & & & & 0 \\ & \ddots & & & & \iddots & \\ & & 0 & 0 & 0 & & \\ & & 0 & 0 & 0 & & \\ & \iddots & -\rho^{-2} & 0 & 1 & & \\ & \iddots & & & & \ddots & \\ 0 & -\rho^{-N+2} & & & & & 1 \end{bmatrix} \hat{a}. \tag{3.2}$$

We denote by $\tilde{P}$, $\tilde{I}$ the lower $\frac{1}{2}N \times \frac{1}{2}N$ blocks in $(\hat{P}-\hat{L})_N$. In order to proceed we need to recall the Gauss doubling formula for the N-point discrete Fourier transform

$$d_\nu = \frac{1}{N}\sum_{j=0}^{N/2-1} \zeta_{2j} w^{-2j\nu} + \frac{1}{N} w^{-\nu} \sum_{j=0}^{N/2-1} \zeta_{2j+1} w^{-2j\nu}, \tag{3.3}$$

for $-\frac{1}{2}N+1 \leqslant \nu \leqslant \frac{1}{2}N$, where $w = e^{i2\pi/N}$. Observe that

$$[F_N]_{k\nu} = w^{-k\nu}, \quad k = 0, \ldots, N-1, \quad \nu = -\tfrac{1}{2}N+1, \ldots, \tfrac{1}{2}N.$$

If, for a vector ζ, we write $\zeta = [\zeta_0, \zeta_1]^{\mathrm{T}}$, where ζ_0 contains the even-index components and ζ_1 those with odd indices, i.e., $\zeta_0 = [\zeta_0, \zeta_2, \ldots, \zeta_{N-2}]^{\mathrm{T}}$ and $\zeta_1 = [\zeta_1, \zeta_3, \ldots, \zeta_{N-1}]^{\mathrm{T}}$, then (3.3) can be written, for $\nu = -\frac{1}{2}N + 1, \ldots, 0$,

$$\begin{bmatrix} d_0 \\ d_{-1} \\ \vdots \\ d_{-N/2+1} \end{bmatrix} = \frac{1}{N} F_{N/2}^{\mathrm{H}} \zeta_0 + \frac{1}{N} W F_{N/2}^{\mathrm{H}} \zeta_1,$$

where H denotes the Hermitian transpose, and $W = \operatorname{diag}(w^0, w^1, \ldots, w^{N/2-1})$; the matrix $F_{N/2}^{\mathrm{H}}$ has components

$$\left[F_{N/2}^{\mathrm{H}}\right]_{kl} = w^{kl}, \quad k, l = 0, \ldots, \tfrac{1}{2}N - 1.$$

(This matrix is denoted by F in [5].) With some additional work we can show also

$$\begin{bmatrix} d_{N/2} \\ \vdots \\ d_1 \end{bmatrix} = \frac{1}{N} F_{N/2}^{\mathrm{H}} \zeta_0 - \frac{1}{N} W F_{N/2}^{\mathrm{H}} \zeta_1.$$

These can be combined into

$$d = \frac{1}{N} F_N \zeta = \frac{1}{N} \begin{bmatrix} F & -WF \\ F & WF \end{bmatrix} \begin{bmatrix} \zeta_0 \\ \zeta_1 \end{bmatrix}, \tag{3.4}$$

where we have written $F = F_{N/2}^{\mathrm{H}}$. If we let $E_0 = \operatorname{diag}(e_0, e_2, \ldots, e_{N-2})$ and $E_1 = \operatorname{diag}(e_1, e_3, \ldots, e_{N-1})$, then (3.1) can be written as

$$\frac{1}{N} \begin{bmatrix} O & O \\ \tilde{P} & \tilde{I} \end{bmatrix} \begin{bmatrix} F & -WF \\ F & WF \end{bmatrix} \begin{bmatrix} E_0 U_0 \\ E_1 U_1 \end{bmatrix} = -\begin{bmatrix} O & O \\ \tilde{P} & \tilde{I} \end{bmatrix} F_N \xi_N = \begin{bmatrix} 0 \\ g \end{bmatrix},$$

that is,

$$\frac{1}{N}(\tilde{I} + \tilde{P}) F E_0 U_0 + \frac{1}{N}(\tilde{I} - \tilde{P}) W F E_1 U_1 = g. \tag{3.5}$$

This is an $\frac{1}{2}N \times \frac{1}{2}N$ system with zeros across the top row. We replace this with the truncation of (2.5), i.e.,

$$p^{\mathrm{T}} F_N E_N U_N = -p^{\mathrm{T}} F_N \xi_N, \tag{3.6}$$

where $p^{\mathrm{T}} = [p_{N/2}, 0, \ldots, p_4, 0, p_2, 0, 1, 0, \ldots, 0]$, and

$$p_{2k} = 2(-1)^k \rho^{-2k}.$$

We denote by P the matrix obtained from $\tilde{P}$ by putting $[p_{N/2}, 0, \ldots, p_2, 0]$ in the first row of $\tilde{P}$. Then (3.5) together with (3.6) can be written

$$\frac{1}{N} A F E_0 U_0 + \frac{1}{N} B F E_1 U_1 = g, \tag{3.7}$$

where $A = I + P$ and $B = (I - P)W$. (We note here that as $\rho \to \infty$, $P \to 0$ and (3.7) becomes [5, (14)].) We will show below that A^{-1} and B^{-1} can be computed explicitly and have the same structure as A and B. If we multiply (3.7) by $E_0^{\mathrm{H}} F^{\mathrm{H}} A^{-1}$, we obtain, using $2F^{\mathrm{H}}F = NI$,

$$U_0 + CU_1 = 2E_0^{\mathrm{H}} F^{\mathrm{H}} A^{-1} g, \tag{3.8}$$

where $C = (2/N) E_0^{\mathrm{H}} F^{\mathrm{H}} A^{-1} BFE_1$. Multiplying (3.8) on the left by C^{-1} yields a similar system. Now, following [8,17], we take real parts of these equations to obtain

$$U_0 + R_1 U_1 = g_0, \qquad R_0 U_0 + U_1 = g_1, \tag{3.9}$$

where $R_1 = \mathrm{Re}\ C$, $R_0 = \mathrm{Re}\ C^{-1}$, $g_0 = 2\mathrm{Re}(E_0^{\mathrm{H}} F^{\mathrm{H}} A^{-1} g)$ and $g_1 = 2\mathrm{Re}(E_1^{\mathrm{H}} F^{\mathrm{H}} B^{-1} g)$. There are a number of possible approaches to solving this (nonsymmetric) system which use the fact that the matrix multiplications can be carried out in $O(N \log N)$ operations using FFTs. We report here results using only one of these; it is similar to a suggestion made in [17]. If we multiply (3.9) by

$$\begin{bmatrix} I & -R_1 \\ O & I \end{bmatrix},$$

we obtain the equivalent system

$$(I - R_1 R_0) U_0 = DU_0 = d = g_0 - R_1 g_1, \qquad R_0 U_0 + U_1 = g_1.$$

We solve the first of these using the conjugate gradient method for the normal equations $D^{\mathrm{T}} D U_0 = D^{\mathrm{T}} d$. The matrix $G = D^{\mathrm{T}} D$ is expected to have one very small eigenvalue corresponding to the expected one-dimensional null space in the infinite-dimensional problem, as discussed in Section 2, and our computations have borne this out. We have dealt with this, following [5], by writing $GU_0 = D^{\mathrm{T}} d = b$ as

$$\begin{bmatrix} g & \hat{g}^{\mathrm{T}} \\ \hat{g} & \hat{G} \end{bmatrix} \begin{bmatrix} u_0 \\ u_2 \\ \vdots \\ u_{N-2} \end{bmatrix} = \begin{bmatrix} b_0 \\ \hat{b} \end{bmatrix},$$

setting $u_0 = 0$, and solving the $(\frac{1}{2}N - 1)$-dimensional system $\hat{G}\hat{U} = \hat{b}$ using conjugate gradient.

We conclude this section with a discussion of the explicit inversion of A and B. Note that

$$A = \begin{bmatrix} a & h^{\mathrm{T}} \\ 0 & \hat{A} \end{bmatrix},$$

where $a = 1 + p_{N/2}$ and $\hat{A} = I - Q$, where Q is a "backward diagonal" matrix with ρ^{-2}, $\rho^{-4}, \ldots, \rho^{-N+2}$ from upper right to lower left. A straightforward calculation shows that

$$\hat{A}^{-1} = (1 - \rho^{-N})^{-1} (I + Q).$$

Then the inverse of A is obtained in the form

$$A^{-1} = \begin{bmatrix} c & g^{\mathrm{T}} \\ 0 & \hat{A}^{-1} \end{bmatrix},$$

where $c = (1 + 2\rho^{-N/2})^{-1}$ and $g^{\mathrm{T}} = -h^{\mathrm{T}}\hat{A}^{-1}/a$. A straightforward calculation shows that

$$g_{2k} = \frac{2(-1)^k \rho^{-2k}\left(1 + (-1)^{N/4-2k}\rho^{-N/2}\right)}{(1 + 2\rho^{-N/2})(1 - \rho^{-N})}$$

and $g_{2k-1} = 0$, $k = 1, \ldots, \frac{1}{4}N$. We can find $B^{-1} = W^{-1}(I - P)^{-1}$ in a similar way.

4. Numerical experiments

We have tested our method for the regions discussed below and found that it works well for regions with aspect ratios up to 10 or 20 to 1 with moderate values of N. This is well beyond what can be achieved with maps from the disk. The application of the method to other and more extreme regions is under study. Our computations were done in double precision on an IBM ES 9000.

Before we discuss the examples, let us give some programming details. The FFT routine we use is the radix-2 complex FFT routine from [1, p.416]. The boundary curves are defined by taking 1000 points γ_i, $i = 1, \ldots, 1000$, along the boundary curve, given by certain analytic formulas and fitting a periodic cubic spline to them parametrized by the chordal approximation to *arc* length between the successive γ_i's according to the algorithm [9]. Thus the regularity of the approximate boundary curve is different than that of the actual boundary curve. The spline fits to the regions are accurate to 10^{-6} or less for the regions below. Also, our regions have $\gamma(0) = 1$ and aspect ratios (minor to major axis ratios) of α, $0 < \alpha \leqslant 1$.

Using the relations between the Chebyshev and the Fourier coefficients, $A_k = 2\rho^{-k}a_k$, $k \geqslant 0$, and (2.1), we have the Laurent series

$$f(\psi(t)) = a_0 + \sum_{k=1}^{\infty} \left(a_k \rho^{-k} t^k + a_{-k}\rho^k t^{-k}\right),$$

for $1 \leqslant |t| \leqslant \rho$. This is a map from the annulus to the target region slit along the image of $|t| = 1$. The discrete version of the sum above can be evaluated at equally spaced points on concentric circles, $|t| =$ constant, using the FFT routines. The plots of the maps in the figures show the images of 5 concentric circles and 32 radial lines in the annulus. The image of $|t| = \rho$ is plotted using $2N$ points. The images of the circles with $|t|$ near 1 often require $\frac{1}{2}N$ or fewer terms to appear at all reasonable. This was particularly true for ρ large.

The aspect ratio for the ellipse is $\alpha = (\rho^2 - 1)/(1 + \rho^2)$. Except for Example 2, we choose α's for the ellipse and for the target curve $\gamma(s)$ to be equal or nearly equal. The mesh points are images of Fourier points under the Joukowski map from the exterior of a disk to the exterior of an ellipse of aspect ratio α. It is easy to see that these mesh points crowd like $O(\alpha)$ at the ends of the major axis. While this may eventually cause difficulties for small α, it is not so severe as the exponential crowding in Example 2; see also [3].

To monitor the outer Newton iterations, we compute the successive iteration error $\max_i |S_{k+1}(\theta_i) - S_k(\theta_i)|$ at the mesh points θ_i, $i = 1, \ldots, N$, the "residual" error

$$\max\left(\max_k |a_{-k} - \rho^{-2k}a_k|, \left|a_0 - 2\rho^{-2}a_2 + 2\rho^{-4}a_4 - \cdots\right|\right);$$

and the exact discretization error $\max_i |f(z_i) - \hat{f}(z_i)|$, when available, at the mesh point z_i, $i = 1, \ldots, N$. Quadratic convergence is observed, but may degrade for the more extreme

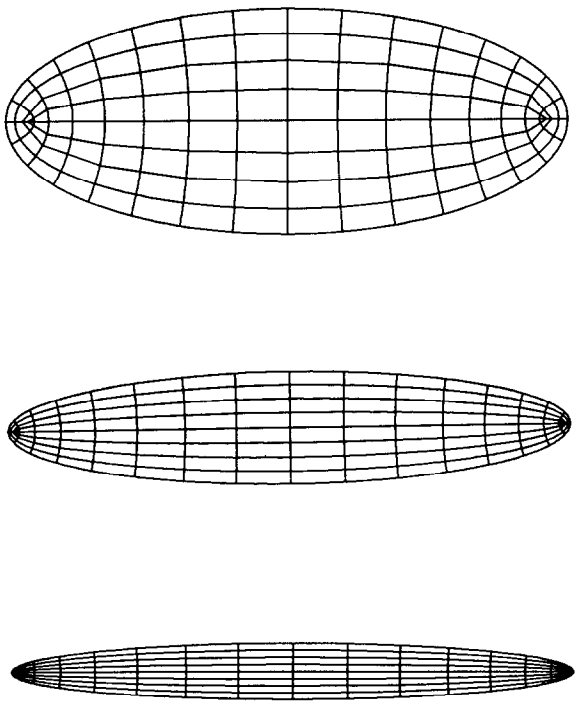

Fig. 1. The identity map for an ellipse to itself with $\alpha = 0.4, 0.2, 0.1$, and $N = 64, 128, 64$, respectively.

regions. The successive iteration errors can often be iterated to 0 ($\sim 10^{-15}$ in double precision), but in some cases the convergence rate may slow after the level of discretization error has been reached and they may then even begin to diverge. This "convergence/divergence" behavior has been observed with Wegmann's method in [3] and discussed in [16]. For our initial guess, we use $S_0(\theta_i)$ proportional to $S(\theta_i)$ for the Joukowski map.

The inner conjugate gradient interations usually converge rapidly, but their convergence rate may also be slower for more extreme cases. We have found it convenient to stop these iterations after either a tolerance of 10^{-15} is achieved or after 10 iterations, which ever comes first. A check of the eigenvalues of $D^{\mathrm{T}}D$ using the NAGLIB routine F02AAF shows that there are usually one or a few small and occasionally negative eigenvalues. The rest are between 0 and 1, mainly near 1 with a few greater than 1. The largest eigenvalue is roughly $1/\alpha$, indicating that the increase in the condition number of $D^{\mathrm{T}}D$ as $\alpha \downarrow 0$ accounts for the slowing of convergence for more slender regions. We plan to investigate the convergence/divergence behavior and the use of alternative solvers for the inner systems, such as GMRES, in the future.

Next, we discuss the examples.

Example 1 (*Ellipse to ellipse*, Fig. 1). This is just the identity map of an ellipse of aspect ratio α to itself. The level of discretization error is reached here in a few iterations and the successive iteration error can usually be driven to 0. The discretization error and residual error increase as $\alpha \downarrow 0$ to, for instance, $\sim 10^{-5}$ for $\alpha = 0.1$. This is about the level of the error in the cubic spline

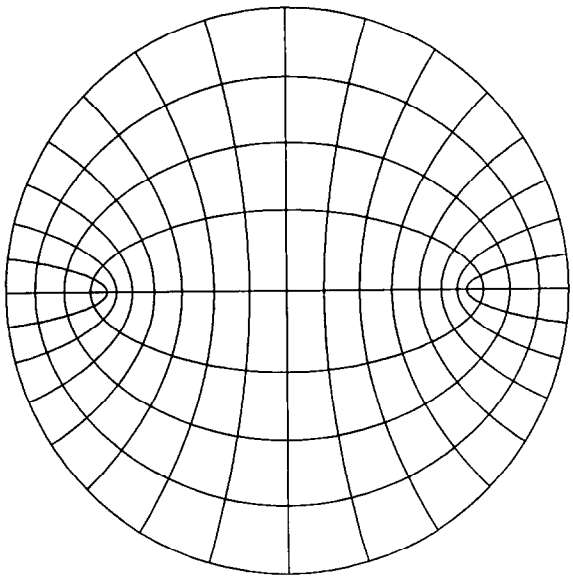

Fig. 2. Map from ellipse $\alpha = 0.8$ to unit disk with $N = 64$.

fit to the target ellipse. Note that all our maps to target regions are scaled so that $f(\pm(\rho + \rho^{-1})) = \pm 1$ and $f(\pm(\rho - \rho^{-1})) = \pm \mathrm{i}\alpha$.

Example 2 (*Ellipse to unit disk*, Figs. 2–4). In this case the exact map is given in [8, p.550] as

$$f(z) = \frac{4}{f'(0)} \sum_{m=0}^{\infty} \frac{(-1)^m T_{2m+1}(z)}{\rho^{4m+2} - \rho^{-4m-2}},$$

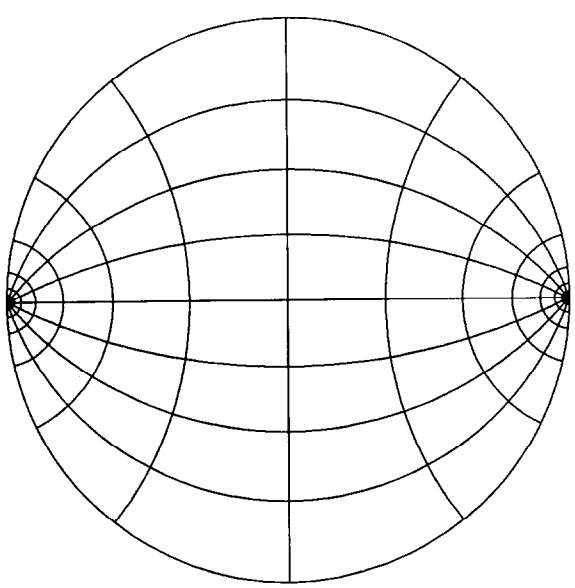

Fig. 3. Map from ellipse $\alpha = 0.4$ to unit disk with $N = 128$.

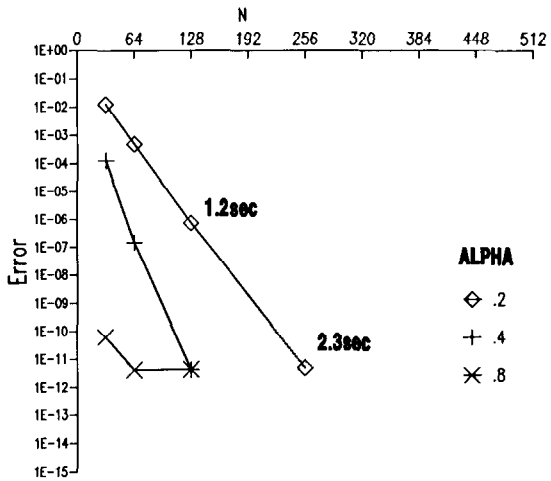

Fig. 4. Discretization error $\max_i |f(z_i) - \hat{f}(z_i)|$ at mesh points z_i for maps from a family of ellipses to the unit disk.

where

$$f'(0) = \left\{ 4 \sum_{m=0}^{\infty} \frac{2m+1}{\rho^{4m+2} - \rho^{-4m-2}} \right\}^{1/2}.$$

(Note that it is easy to check that the Laurent coefficients satisfy (2.1) in this case.) In this case there is severe exponential crowding of the mesh points near ± 1. The successive iteration error converges to about 10^{-13} and then starts to diverge. The discretization error is displayed in Fig. 4. It behaves like $O(R^{-N})$ as would be expected for an analytic boundary curve with $R = R(\alpha)$ the modulus of the nearest singularity $R > \rho$. For $\alpha = 0.8$, $N = 64$ and 128, the error remains constant. This is approximately the error in the cubic spline fit to the disk. Replacing the analytic parametrization of the boundary by a cubic spline parametrization does not destroy the effects of the underlying regularity of the boundary, at least not up to the level of error in the fit. This is also observed in the next example and in experiments in [2] with Wegmann's method.

Example 3 (*Ellipse to arctanh region*, Fig. 5). The map $f(z) = \operatorname{arctanh}(rz) = \frac{1}{2}\log(1 + rz)/(1 - rz)$, $0 < r \leqslant 1$, maps the unit disk to a slender region (the infinite channel for $r = 1$). This is a standard example of a difficult map for Fourier series methods on the disk. It is easy to show that $|f'(\pm 1)|$ grows exponentially with aspect ratio $\alpha \downarrow 0$ $(r \uparrow 1)$, so that the images of the Fourier points do not resolve the boundary near $f(\pm 1)$ very well even with very large N. Composing this map with the map in Example 2 from an ellipse of similar aspect ratio to the disk provides us with an exact map for this test case. The discretization error is given in Fig. 6. Since the boundary is analytic, the error again behaves like $O(R^{-N})$ until the error in the spline fit is reached at $\sim 10^{-6}$. For comparison, with Wegmann's method, the map from the disk to the arctanh region with $\alpha = 0.29$ $(r = 0.99)$ requires $N = 1024$ for an error of $\sim 10^{-4}$ and many iterations (6.0 CPU-seconds), whereas our method achieved 10^{-6} accuracy with $N = 64$ in 0.6 sec. (We have used a parametrization of the boundary, $(1 + r^2)\cos y = (1 - r^2)\cosh x$, provided by John Pfaltzgraff, to distribute knots for the spline along the boundary.) The successive iteration errors could often be decreased to $\sim 10^{-15}$ if enough iterations were taken here.

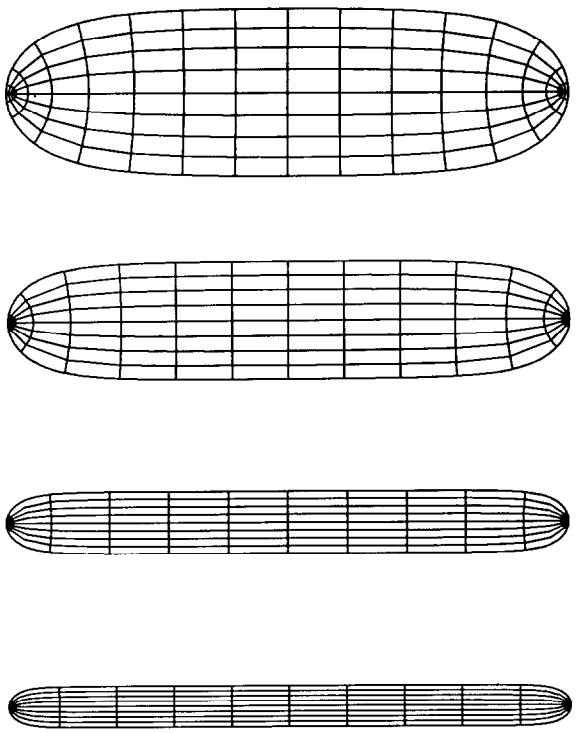

Fig. 5. Maps for the arctanh region with $\alpha = 0.29, 0.206, 0.108, 0.073$, and $N = 128, 128, 256, 512$, respectively.

Example 4 (*Ellipse to sports ground*, Fig. 7). This region of length 2 is bounded by two semicircles of radius α connected by horizontal line segments. Thus the boundary here is C^1; however, it is then approximated by a cubic spline. In Fig. 8, the residual error is displayed. It behaves roughly like $O(N^{-3})$. Some convergence/divergence behavior is seen.

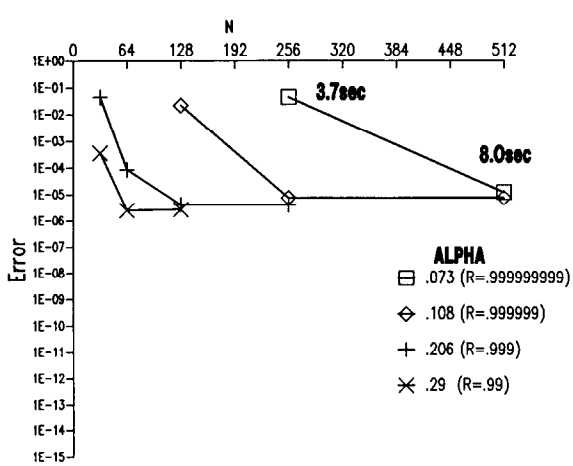

Fig. 6. Discretization error $\max_i |f(z_i) - \hat{f}(z_i)|$ at the mesh points z_i for maps from ellipses $\alpha = 0.3, 0.2, 0.1, 0.07$ to arctanh regions $\alpha = 0.29, 0.206, 0.108, 0.073$, respectively.

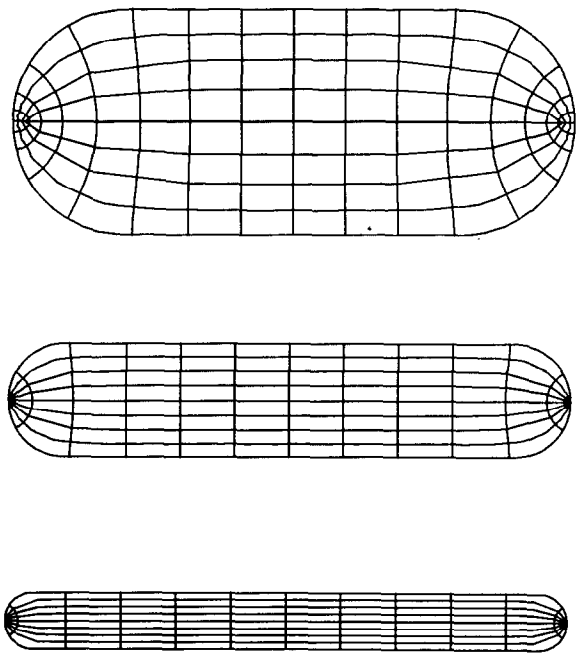

Fig. 7. Map from ellipse to sports ground with $\alpha = 0.4, 0.2, 0.1$ (both regions), and $N = 64, 128, 512$.

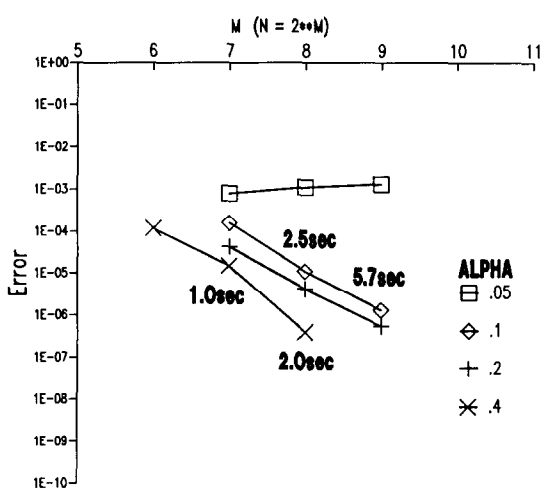

Fig. 8. Residual error $\max_k |a_{-k} - \rho^{-2k} a_k|$ in Laurent coefficients a_k for maps from ellipse to sports ground.

Fig. 9. Map from ellipse with $\alpha = 0.1$ to a spline curve, $N = 128$.

Example 5 (*Ellipse to spline curve*, Fig. 9). In this example we construct the map from an ellipse with $\alpha = 0.1$ to a slender "wavy" region produced by taking several points in the plane and fitting them with our spline routine. With $N = 128$ both the successive iteration error and the residual error decreased to less than 10^{-5} in four iterations.

5. Remarks

We have used only one of many possible methods for solving the (finite-dimensional) system in a Newton update. We plan to investigate others, in particular some of the generalizations of conjugate gradient to nonsymmetric systems such as GCR or GMRES. Our solution using conjugate gradient for the normal equations has the potential of degrading the convergence properties, but we have not had serious difficulties with this in our computations.

The infinite-dimensional system discussed in Section 2 can be written in terms of integral operators, following [15,17], and the operators are compact. It should be possible to study the spectra of the integral operator and explain the behavior of the conjugate gradient method observed in Section 4. The details are more complicated than in [15], however; we have not succeeded in writing the updates explicitly in terms of a Riemann–Hilbert problem, for example.

We expect that it can be proven that crowding in the map from an appropriate ellipse to a slender region is not too large, and that the obvious initial guess for Newton's method is close enough for convergence. (We have in mind, in particular, [12, Theorem 5.1].) In a similar way we believe that results from approximation theory should enable us to show a Zemach-like rule [2,18] to the effect that $N \sim \| f' \|_\infty$ for a reasonable approximation.

An immediate application of this method is to translate Dirichlet problems for harmonic functions to the ellipse and solve them with Chebyshev series; see, for example, [11]. A formula for the Dirichlet integral can be derived in terms of Chebyshev coefficients, and this is potentially useful in solving resolution difficulties that we have experienced in solving free boundary problems using conformal mapping (cf. [4]).

Finally, we remark on using the ideas here for domains which are slender in more than one direction, a cross, for example. On the face of it, our method depends on explicit properties of the Joukowski map and its Faber polynomials. On the other hand, for any curve for which the exterior map is known and the Faber polynomials can be generated conveniently, much of the above can be carried through, at least in principle. In particular, an operator equation expressed in terms of Fourier coefficients of a transplanted function can be used to express analytic extendibility of a function. It would be interesting to see how far this can be carried through in practice.

Acknowledgement

The authors thank John Pfaltzgraff for useful discussions.

References

[1] G. Dahlquist and A. Björck, *Numerical Methods* (Prentice-Hall, Englewood Cliffs, NJ, 1974).

[2] T.K. DeLillo, The accuracy of numerical conformal mapping methods. A survey of examples and results, preprint.

[3] T.K. DeLillo and A.R. Elcrat, A comparison of some numerical conformal mapping methods for exterior regions, *SIAM J. Sci. Statist. Comput.* **12** (1991) 399–442.

[4] T.K. DeLillo, A.R. Elcrat and K.G. Miller, Constant vorticity Riabouchinsky flows from a variational principle, *Z. Angew. Math. Phys.* **41** (1990) 755–765.

[5] B. Fornberg, A numerical method for conformal mappings, *SIAM J. Sci. Statist. Comput.* **1** (1980) 386–400.

[6] D. Gaier, *Konstruktive Methoden der Konformen Abbildung* (Springer, Berlin, 1964).

[7] K.O. Geddes, Near-minimax polynomial approximation in an elliptical region, *SIAM J. Numer. Anal.* **15** (1978) 1225–1233.

[8] P. Henrici, *Applied and Computational Complex Analysis, Vol. 3* (Wiley, New York, 1986).

[9] W.D. Hoskins and P.R. King, Periodic cubic spline interpolation using parametric splines, Algorithm 73, *Computer J.* **15** (1972) 282–283.

[10] L.H. Howell and L.N. Trefethen, A modified Schwarz–Christoffel transformation for elongated regions, *SIAM J. Sci. Statist. Comput.* **11** (1990) 928–949.

[11] W.C. Royster, A Poisson integral formula for the ellipse and some applications, *Proc. Amer. Math. Soc.* **15** (1964) 661–670.

[12] S. Warschawski, On conformal mapping of a variable region, in: F. Beckenbach, Ed., *Constructions and Applications of Conformal Maps*, Nat. Bureau Standards Appl. Math. Ser. **18** (U.S. Government Printing Office, Washington, DC, 1952) 175–187.

[13] R. Wegmann, Ein Iterationsverfahren zur konformen Abbildung, *Numer. Math.* **30** (1978) 453–466; translated as: An iterative method for conformal mapping, in: L.N. Trefethen, Ed., *Numerical Conformal Mapping* (North-Holland, Amsterdam, 1986) 7–18; also: *J. Comput. Appl. Math.* **14** (1&2) (1986) 7–18.

[14] R. Wegmann, Convergence proofs and error estimates for an iterative method for conformal mapping, *Numer. Math.* **44** (1984) 435–461.

[15] R. Wegmann, On Fornberg's numerical method for conformal mapping, *SIAM J. Numer. Anal.* **23** (1986) 1199–1213.

[16] R. Wegmann, Discretized versions of Newton type iterative methods for conformal mapping, *J. Comput. Appl. Math.* **29** (2) (1990) 207–224.

[17] O. Widlund, On a numerical method for conformal mapping due to Fornberg, unpublished.

[18] C. Zemach, A conformal map formula for difficult cases, in: L.N. Trefethen, Ed., *Numerical Conformal Mapping* (North-Holland, Amsterdam, 1986) 207–215; also: *J. Comput. Appl. Math.* **14** (1&2) (1986) 207–215.